Volume 14 | Number 22 | 21 November 2014 | Pages 4297–4436

Lab on a Chip

Miniaturisation for chemistry, physics, biology, materials science and bioengineering

www.rsc.org/loc

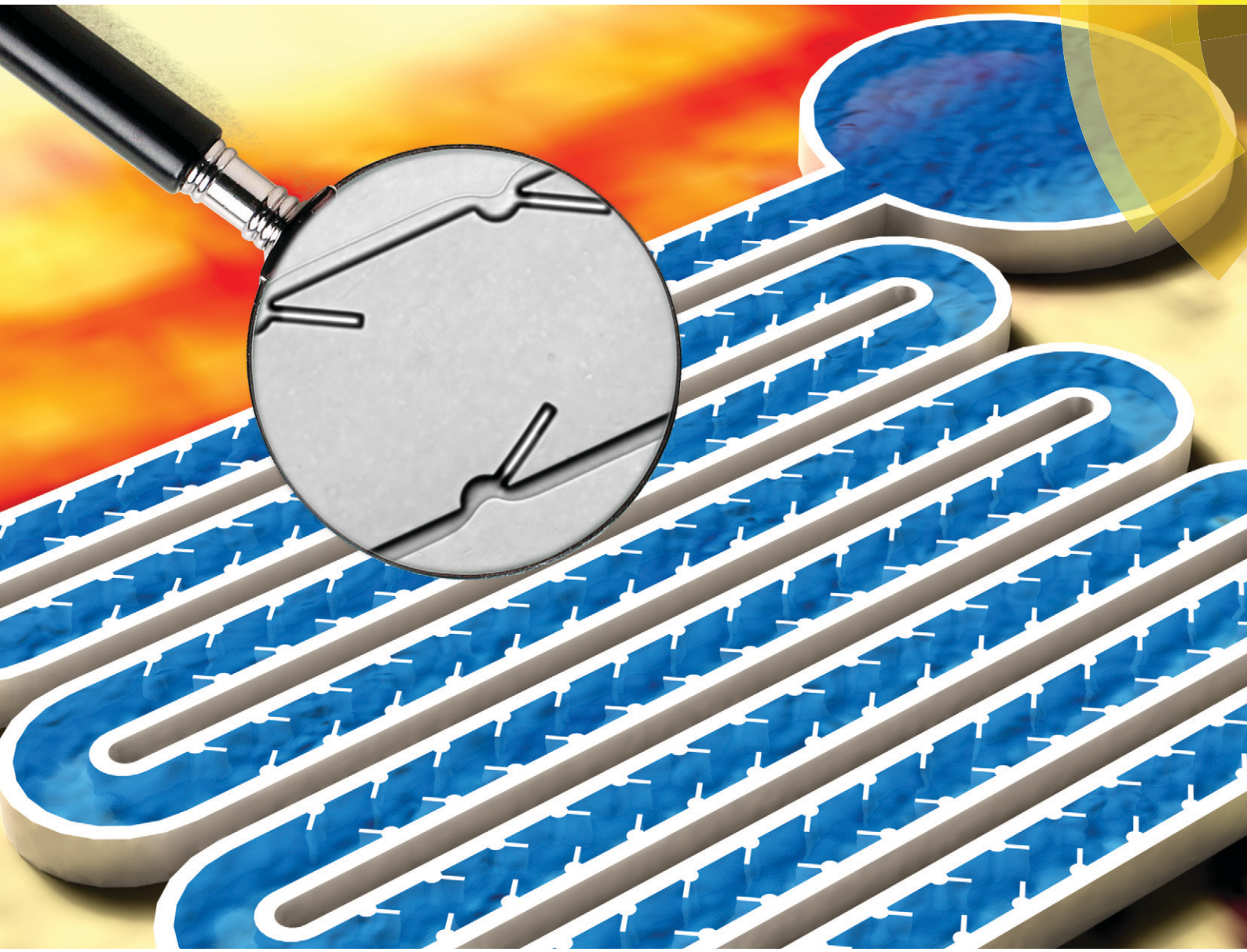

ISSN 1473-0197

ROYAL SOCIETY OF CHEMISTRY

COMMUNICATION

Tony Jun Huang *et al.*

A reliable and programmable acoustofluidic pump powered by oscillating sharp-edge structures

Lab on a Chip

COMMUNICATION

View Article Online
View Journal | View Issue

Cite this: *Lab Chip*, 2014, **14**, 4319

Received 10th July 2014,
Accepted 18th August 2014

DOI: 10.1039/c4lc00806e

www.rsc.org/loc

A reliable and programmable acoustofluidic pump powered by oscillating sharp-edge structures†

Po-Hsun Huang,[a] Nitesh Nama,[a] Zhangming Mao,[a] Peng Li,[a] Joseph Rufo,[a] Yuchao Chen,[a] Yuliang Xie,[ac] Cheng-Hsin Wei,[b] Lin Wang[d] and Tony Jun Huang*[ac]

We present a programmable acoustofluidic pump that utilizes the acoustic streaming effects generated by the oscillation of tilted sharp-edge structures. This sharp-edge-based acoustofluidic pump is capable of generating stable flow rates as high as 8 μL min^{-1} (~76 Pa of pumping pressure), and it can tune flow rates across a wide range (nanoliters to microliters per minute). Along with its ability to reliably produce stable and tunable flow rates, the acoustofluidic pump is easy to operate and requires minimum hardware, showing great potential for a variety of applications.

In the past two decades, significant efforts have been made towards developing reliable and robust microfluidic pumps.[1–3] These microfluidic pumps can be generally divided into two categories based on their driving mechanisms: passive pumps[4–6] and active pumps.[7–9] Passive pumps, particularly the surface-tension-based microfluidic pumps,[10,11] allow the manipulation of fluids without the need of peripheral equipment or moving parts, making them suitable to many portable analytical devices. Nevertheless, they are incapable of performing complex fluid manipulations as the flow direction and flow rate cannot be adjusted in real time and on demand, preventing their use in applications where multiple steps of fluid operations (*e.g.*, immunoassay) are required. In contrast, active pumps, which use mechanical or electrical actuations, or other external forces to initiate fluid pumping, offer much more flexibility in terms of fluid manipulations and can potentially provide solutions to the challenges faced by passive pumps.

Many active microfluidic pumps have been reported, including optically driven pumps,[12,13] electroosmotic pumps,[14,15] electrokinetic pumps,[16,17] dielectric pumps,[18,19] magnetic pumps,[20,21] laser-driven pumps,[22] pneumatic membrane pumps,[23–25] bio-hybrid pumps,[26,27] and diffuser pumps.[28,29] Despite these advances, the existing active micropumps suffer from drawbacks such as complicated device fabrication, involvement of moving structures, and/or unstable and unreliable performance. Recently, implementation of acoustic streaming effects[29] in microfluidics has attracted great interest and enabled numerous applications, including mixing,[30–34] particle manipulation,[35–39] and flow control.[40,41] Microfluidic pumps powered by acoustically oscillating microbubbles have also been demonstrated.[42,43] These bubble-based pumps are simple to fabricate and operate; however, the performance of these pumps suffers from bubble instability, temperature dependence, and inconvenience of the bubble-trapping process.

In this communication, we establish a simple and reliable microfluidic pumping mechanism using acoustically driven solid sidewall microstructures known as "sharp edges". This work is built upon our previous finding that acoustic streaming effects can be induced by acoustically oscillating sharp edges.[44,45] With the acoustically induced acoustic streaming effects, we previously demonstrated rapid and homogeneous fluid mixing inside a microfluidic channel.[44] In this work, we redesign the geometry and orientation of the sharp-edge structures and demonstrate that the sharp-edge-induced acoustic streaming can lead to applications beyond mixing. In particular, we demonstrate a highly effective, reliable, and programmable microfluidic pump with minimum hardware. Our sharp-edge-based acoustofluidic micropump can generate a flow rate of approximately 8 μL min^{-1}, which corresponds to a pumping pressure of 76 Pa. Moreover, it is capable of generating flow rates ranging from nanoliters to microliters per minute – a capability that most existing microfluidic pumps do not possess. Our acoustofluidic pump can be operated on demand and features advantages,

[a] *Department of Engineering Science and Mechanics, The Pennsylvania State University, University Park, PA 16802, USA. E-mail: junhuang@psu.edu*
[b] *Department of Nutritional Sciences, The Pennsylvania State University, University Park, PA 16802, USA*
[c] *Department of Chemical Engineering, The Pennsylvania State University, University Park, PA 16802, USA*
[d] *Ascent Bio-Nano Technologies Inc., State College, PA 16802, USA*

† Electronic supplementary information (ESI) available: Video 1: pumping behavior under different voltages. Video 2: pulsed pumping behavior. See DOI: 10.1039/c4lc00806e

such as simple fabrication and operation, high reliability, compactness, and tunable flow rates without complicated moving parts.

Fig. 1 schematically shows the design and working mechanism of our acoustofluidic pump. Briefly, the acoustofluidic pump was made by bonding a single-layer polydimethylsiloxane (PDMS) channel onto a single glass slide and attaching a piezoelectric transducer (part no. 81-7BB-27-4L0, Murata Electronics) adjacent to it using a thin layer of epoxy (PermaPoxy™ 5 Minute General Purpose, Permatex). To demonstrate the pumping behavior, the PDMS channel was designed to be a rectangular recirculating (in a counter-clockwise direction) channel composed of four portions: left channel, right channel, upper channel, and lower channel. The lower channel, referred to as the pumping region, was designed with 20 tilted sharp-edge structures on its sidewall (10 on each side), while the other three channels were straight channels without any structures. The piezoelectric transducer, activated by amplified sine wave signals from a function generator (AFG3011C, Tektronix) and an amplifier (25A250A, Amplifier Research), was used to acoustically oscillate the sharp-edge structures to generate acoustic streaming effects. As shown in Fig. 1b, the tilted sharp-edge structure, acoustically oscillated by the activation of the piezoelectric transducer, generates an acoustic streaming pattern around its tip; since the sharp edges are tilted to the right, the streaming results in a net force directed to the right. Fluid pumping occurs because the generated net forces push the bulk fluid. Fig. 1c shows the design of our acoustofluidic device. The microchannel has a width of 600 μm and a depth of 100 μm, and each sharp-edge structure is identical. Different tilting angles (α) of the sharp-edge structures, including 30°, 45°, 60°, and 70°, were chosen to investigate the resulting pumping behavior and determine the best angle for optimal pumping performance.

To prove our concept and determine the working frequency of the piezoelectric transducer, the pumping device with 30° tilted sharp-edge structures was experimentally and numerically tested first. A solution containing DI water and dragon green fluorescent beads (Bangs Laboratory) with a diameter of 1.9 μm was injected into the channel to characterize the acoustic streaming patterns induced by the oscillation of tilted sharp-edge structures. After injecting the solution, the inlet/outlet ports were sealed by two separate tubes connected to two separate syringes, such that no pressure difference is present between the inlet and the outlet. By sweeping the frequency with a 50 Hz increment from 1 kHz to 100 kHz, we observed that the acoustic streaming patterns were developed around the tips of the oscillating sharp-edge structures when the piezoelectric transducer was activated at 6.5 kHz, as shown in Fig. 2a. Based on these results, 6.5 kHz appeared to be the working frequency for the piezoelectric transducer to activate our pump. As a result, we used this frequency for all of the following experiments. Additionally, using the simulation approach we reported recently[45] to model the acoustically driven oscillating 30° tilted sharp-edge structures shown in Fig. 2b, we found that the acoustic streaming effects produce a net flow of the fluid from left to right. These simulation results indicate pumping behavior and are also in good agreement with the experimental results

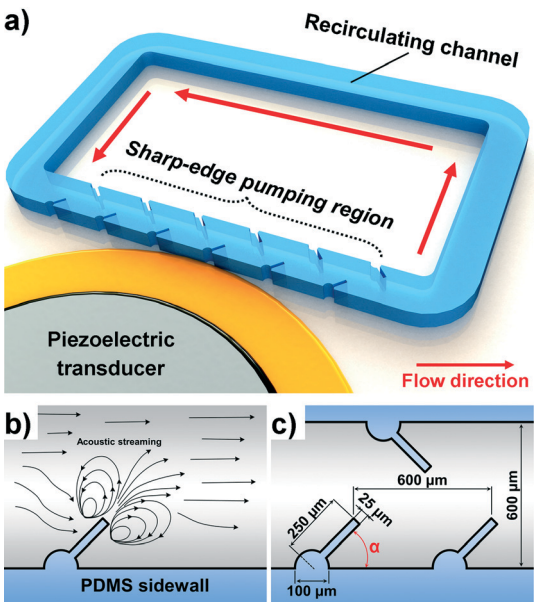

Fig. 1 (a) Schematic of the sharp-edge-based acoustofluidic pumping device. This device includes a PDMS microfluidic channel and a piezoelectric transducer. (b) Schematic showing the acoustic streaming phenomenon around the tip of a tilted oscillating sharp-edge structure. (c) Schematic showing the design of the channel and sharp-edge structure.

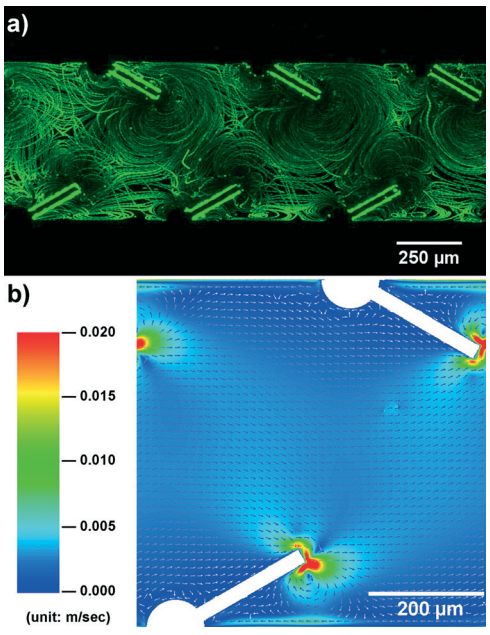

Fig. 2 (a) Characterization of the acoustic streaming patterns developed around the tips of the 30° tilted sharp-edge structures. (b) Simulated results showing the streaming velocity in our pump in the presence of an acoustic field: a net flow of fluid from left to right is generated.

we acquired. It should also be noted that in the simulations a flow singularity was observed at the sharp edges, similar to that observed in our previous study,[45] which is indicated by the maximum velocity at the sharp edge tips. This velocity increases with the mesh refinement and our solution is strictly valid only outside the boundary layer.

To further visualize and characterize the pumping behavior, DI water mixed with polystyrene beads of different diameters (10 μm and 0.9 μm) was injected into the channel. Fig. 3 shows the movement of polystyrene beads over time in the upper channel when the piezoelectric transducer was on (input voltage applied to the piezoelectric transducer = 20 V_{PP}), using the pumping device with 30° tilted sharp-edge structures. The results reveal that with the piezoelectric transducer activated, the representative groups of the beads (circled in red, yellow and blue) were moving from right to left, showing evidence that the fluid was being pumped and flowing along the recirculating channel.

After proving the proposed pumping concept and determining the working frequency for the piezoelectric transducer, we further investigated the influence of the tilting angle of sharp-edge structures on the pumping performance. To quantitatively do so, we estimated the average flow rate inside the channel. The average flow rate was calculated by tracking the average velocities of 10 μm beads in the upper channel, in which ~100 beads were randomly selected and tracked for each independent experiment. In addition to the effect of the tilting angle, pumping performance under different input voltages of the piezoelectric transducer was also characterized. Fig. 4a shows the pumping performance for the four different tilting angles of sharp-edge structures under different input voltages. The results show that when the piezoelectric transducer was activated with voltages ranging from 5 V_{PP} to 50 V_{PP}, pumping took place in all of the devices, regardless of the tilting angle of the sharp-edge structures. As the tilting angle decreased, the generated pumping flow rate increased. As shown in Fig. 4a, of the four different tilting angles, the device with 30° tilted sharp-edge structures generated a significantly larger pumping flow rate, and with a voltage of 50 V_{PP}, it generated a flow rate as high as 8 μL min^{-1}. Using Poiseuille's law[43] and considering the channel length (25 mm), this flow rate corresponds to a calculated pumping pressure of 76 Pa. The lower pumping flow rates generated by the 45°, 60°, and 70° tilted sharp-edge structures can be attributed to the fact that as the tilting angle increases, the component of the generated net force that is perpendicular to the flow direction also increases. As a result, the parallel component of the force that could push the bulk fluid to flow forward is decreased. Further work including different geometries of sharp-edge structure with

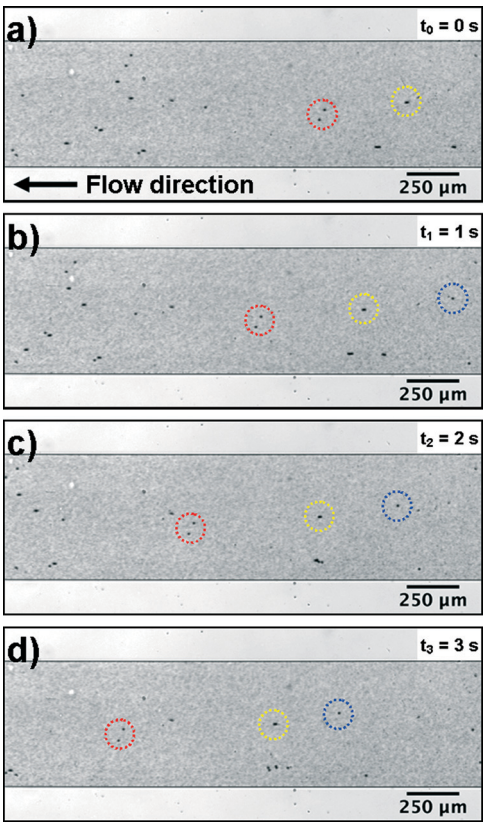

Fig. 3 Experimental images showing the pumping behavior by indicating the movement of polystyrene beads at different time frames when (a) t_0 = 0 s, (b) t_1 = 1 s, (c) t_2 = 2 s, and (d) t_3 = 3 s (red, yellow, and blue circles indicate three representative groups of beads).

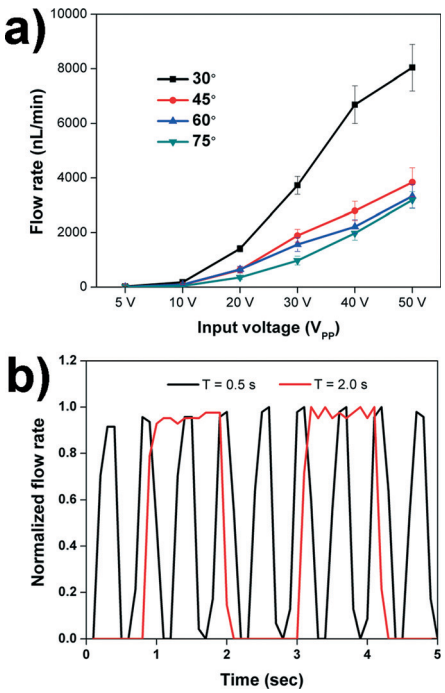

Fig. 4 Experimental results illustrating the controllability and tunability of our acoustofluidic pump. (a) Comparison of generated pumping flow rates with various tilting angles of sharp-edge structures as a function of the voltages applied to the piezoelectric transducer. The 30° tilted sharp-edge structures could generate a flow rate as high as 8 μL min^{-1} under 50 V_{PP}. (b) Characterization of flow rate profiles by alternately switching the piezoelectric transducer on and off with different burst frequencies: burst frequency of 2 Hz (black) and burst frequency of 0.5 Hz (red).

smaller tilting angles to further improve the efficiency of our acoustofluidic pumps is under way. In addition, the results show a concurrent increase of the flow rate with voltage, demonstrating that the pumping flow rate could be controlled by adjusting the input voltages.

We discovered that our acoustofluidic pumps can conveniently achieve a wide range of pumping flow rates, from nanoliters to microliters per minute, by adjusting the input voltage applied to the piezoelectric transducer. Video 1 in the ESI† shows the real-time pumping behavior using the pumping device with 30° tilted sharp-edge structures under different voltages. Aside from the function of continuous fluid pumping, we also demonstrated (Fig. 4b) that by alternately switching the piezoelectric transducer on and off at various burst frequencies (*e.g.*, 0.5 and 2 Hz), our acoustofluidic pump can achieve pulsatile fluid pumping. These results imply that the profile of the pumping flow rate can possibly be modulated by programming the input signal to the piezoelectric transducer. A video showing the pulsed pumping behavior can be found in the ESI† (Video 2). Future work should include evaluation and optimization of pumping performance within different microchannel designs (*e.g.*, a straight, non-circulating microchannel).

In summary, we demonstrate a new class of acoustically driven, reliable, and programmable microfluidic pumps based on the oscillating tilted sharp-edge structures. Our acoustofluidic pump could generate a pumping flow rate as high as 8 $\mu L\ min^{-1}$, and with more sharp-edge structures, the generation of higher flow rates can be expected. By tuning the input voltage, a wide range of pumping flow rates, from nanoliters to microliters per minute, could also be generated by a single pump. Moreover, by programming the input signal to the piezoelectric transducer, we could modulate the profiles of the pumping flow rates. In fact, it is possible to achieve various kinds of flow operations by programming the input signals to the piezoelectric transducer. With such features, our acoustofluidic pump offers advantages over other microfluidic pumps in terms of not only simplicity, stability, reliability, and cost-effectiveness but also controllability and flexibility, which, when combined, make it valuable in many lab-on-a-chip applications.

Acknowledgements

This research was supported by the National Institutes of Health (Director's New Innovator Award, 1DP2OD007209-01), the National Science Foundation (CBET-1438126 and IIP-1346440), and the Penn State Center for Nanoscale Science (MRSEC) under grant DMR-0820404. Components of this work were conducted at the Penn State node of the NSF-funded National Nanotechnology Infrastructure Network.

References

1 B. D. Iverson and S. V. Garimella, *Microfluid. Nanofluid.*, 2008, **5**, 145–174.
2 A. K. Au, H. Lai, B. R. Utela and A. Folch, *Micromachines*, 2011, **2**, 179–220.
3 H. Lai and A. Folch, *Lab Chip*, 2011, **11**, 336–342.
4 M. Zimmermann, H. Schmid, P. Hunziker and E. Delamarche, *Lab Chip*, 2007, **7**, 119–125.
5 S.-H. Chao and D. R. Meldrum, *Lab Chip*, 2009, **9**, 867–869.
6 G. M. Walker and D. J. Beebe, *Lab Chip*, 2002, **2**, 131–134.
7 M. A. Unger, H. P. Chou, T. Thorsen, A. Scherer and S. R. Quake, *Science*, 2000, **288**, 113–116.
8 A. Brask, D. Snakenborg, J. P. Kutter and H. Bruus, *Lab Chip*, 2006, **6**, 280–288.
9 S. Huang, C. Li and J. Qin, *Lab Chip*, 2010, **10**, 2925–2931.
10 P. J. Resto, E. Berthier, D. J. Beebe and J. C. Williams, *Lab Chip*, 2012, **12**, 2221–2228.
11 E. Berthier and D. J. Beebe, *Lab Chip*, 2007, **7**, 1475–1478.
12 J. Leach, H. Mushfique, R. di Leonardo, M. Padgett and J. Cooper, *Lab Chip*, 2006, **6**, 735–739.
13 S. Maruo and H. Inoue, *Appl. Phys. Lett.*, 2007, **91**, 084101.
14 C. Wang, L. Wang, X. Zhu, Y. Wang and J. Xue, *Lab Chip*, 2012, **12**, 1710–1716.
15 M. Gao and L. Gui, *Lab Chip*, 2014, **14**, 1866–1872.
16 M. Bazant and T. Squires, *Phys. Rev. Lett.*, 2004, **92**, 066101.
17 M. M. Gregersen, A. Brask, M. F. Hansen and H. Bruus, *Phys. Rev. E: Stat., Nonlinear, Soft Matter Phys.*, 2007, **76**, 056305.
18 H. Ren, S. Xu and S.-T. Wu, *Lab Chip*, 2013, **13**, 100–105.
19 S.-K. Fan, W.-J. Chen, T.-H. Lin, T.-T. Wang and Y.-C. Lin, *Lab Chip*, 2009, **9**, 1590–1595.
20 J. Atencia and D. J. Beebe, *Lab Chip*, 2004, **4**, 598–602.
21 B. A. Malouin, M. J. Vogel, J. D. Olles, L. Cheng and A. H. Hirsa, *Lab Chip*, 2011, **11**, 393–397.
22 Y. Chen, T.-H. Wu and P.-Y. Chiou, *Lab Chip*, 2012, **12**, 2–5.
23 H.-Y. Tseng, C.-H. Wang, W.-Y. Lin and G.-B. Lee, *Biomed. Microdevices*, 2007, **9**, 545–554.
24 Y.-N. Yang, S.-K. Hsiung and G.-B. Lee, *Microfluid. Nanofluid.*, 2008, **6**, 823–833.
25 H. Chen, J. Cornwell, H. Zhang, T. Lim, R. Resurreccion, T. Port, G. Rosengarten and R. E. Nordon, *Lab Chip*, 2013, **13**, 2999–3007.
26 J. Park, I. C. Kim, J. Baek, M. Cha, J. Kim, S. Park, J. Lee and B. Kim, *Lab Chip*, 2007, **7**, 1367–1370.
27 H. Andersson, W. Van Der Wijngaart, P. Nilsson, P. Enoksson and G. Stemme, *Sens. Actuators, B*, 2001, **72**, 259–265.
28 N. Nguyen and X. Huang, *Sens. Actuators, A*, 2001, **88**, 104–111.
29 H. Bruus, J. Dual, J. Hawkes, M. Hill, T. Laurell, J. Nilsson, S. Radel, S. Sadhal and M. Wiklund, *Lab Chip*, 2011, **11**, 3579–3580.
30 D. Ahmed, X. Mao, B. K. Juluri and T. J. Huang, *Microfluid. Nanofluid.*, 2009, **7**, 727–731.
31 D. Ahmed, X. Mao, J. Shi, B. K. Juluri and T. J. Huang, *Lab Chip*, 2009, **9**, 2738–2741.
32 D. Ahmed, C. Y. Chan, S.-C. S. Lin, H. S. Muddana, N. Nama, S. J. Benkovic and T. J. Huang, *Lab Chip*, 2013, **13**, 328–331.
33 P.-H. Huang, M. I. Lapsley, D. Ahmed, Y. Chen, L. Wang and T. J. Huang, *Appl. Phys. Lett.*, 2012, **101**, 141101.

34 G. Destgeer, S. Im, B. H. Ha, J. H. Jung, M. A. Ansari and H. J. Sung, *Appl. Phys. Lett.*, 2014, **104**, 023506.
35 P. Rogers and A. Neild, *Lab Chip*, 2011, **11**, 3710–3715.
36 L. Schmid, D. A. Weitz and T. Franke, *Lab Chip*, 2014, **14**, 3710–3718.
37 G. Destgeer, K. H. Lee, J. H. Jung, A. Alazzam and H. J. Sung, *Lab Chip*, 2013, **13**, 4210–4216.
38 X. Ding, P. Li, S.-C. S. Lin, Z. S. Stratton, N. Nama, F. Guo, D. Slotcavage, X. Mao, J. Shi, F. Costanzo and T. J. Huang, *Lab Chip*, 2013, **13**, 3626–3649.
39 S.-C. S. Lin, X. Mao and T. J. Huang, *Lab Chip*, 2012, **12**, 2766–2770.
40 L. Schmid, A. Wixforth, D. A. Weitz and T. Franke, *Microfluid. Nanofluid.*, 2011, **12**, 229–235.
41 A. Hashmi, G. Heiman, G. Yu, M. Lewis, H.-J. Kwon and J. Xu, *Microfluid. Nanofluid.*, 2012, **14**, 591–596.
42 A. R. Tovar and A. P. Lee, *Lab Chip*, 2009, **9**, 41–43.
43 A. R. Tovar, M. V. Patel and A. P. Lee, *Microfluid. Nanofluid.*, 2011, **10**, 1269–1278.
44 P.-H. Huang, Y. Xie, D. Ahmed, J. Rufo, N. Nama, Y. Chen, C. Y. Chan and T. J. Huang, *Lab Chip*, 2013, **13**, 3847–3852.
45 N. Nama, P.-H. Huang, T. J. Huang and F. Costanzo, *Lab Chip*, 2014, **43**, 2824–2836.